D/H variation in terrestrial lipids from Santa Barbara Basin over the past 1400 years: A preliminary assessment of paleoclimatic relevance

Chao Li [a,*], Alex L. Sessions [a], David L. Valentine [b], Nivedita Thiagarajan [a]

[a] Division of Geological and Planetary Sciences, California Institute of Technology, MC 100-23, Pasadena, CA 91125, USA
[b] Department of Earth Sciences, University of California, Santa Barbara, CA 93106, USA

ABSTRACT

We analyzed D/H ratios of common terrestrial leaf wax lipids in a 1400 year sediment core from the Santa Barbara Basin (SBB) to test whether they accurately record terrestrial climate in Southern California. The D/H ratios of long chain n-alkanes vary substantially with depth, but are poorly correlated with other terrestrial climate proxies. Interference from fossil hydrocarbons may be at least partly responsible. Long chain n-alkanoic acids exhibit nearly constant downcore D/H ratio values. This constancy in the face of known climatic shifts presumably reflects a substantial residence time for leaf wax compounds in terrestrial soil and/or on the basin flanks. Alternatively, the isotopic composition of meteoric waters in Southern California may not covary with climate, particularly aridity. However, the δD values of n-C_{22} and n-C_{24} fatty acids, commonly attributed to terrestrial aquatic sources, are partially correlated with Southern California winter Palmer Drought Severity Index, a tree ring-based climatic proxy (R^2 0.25; $p < 0.01$) on multi-centennial scales with an inferred ca. 215 year time lag. The improved correlation of these biomarkers can be explained by the fact that they are not stored in terrestrial soil nor are subject to interference from fossil hydrocarbons. Our study indicates that the SBB is unlikely to preserve high resolution leaf wax D/H records that can serve as quantitative paleoclimate proxies, though some qualitative information may be retained. More generally, the sources of lipids in marginal marine basins need to be carefully evaluated prior to attempting paleoclimate reconstruction based on the leaf wax D/H proxy.

© 2010 Elsevier Ltd. All rights reserved.

1. Introduction

Southern California is currently home to ca. 24 million people. With a mean annual precipitation of <600 mm, fresh water is perhaps the most critical natural resource for the region. Most regional climate assessments suggest that the region will continue to dry further (e.g. Barnett et al., 2008; Overpeck and Udall, 2010) with future anthropogenic warming, although the magnitude of such changes is uncertain. To enable adequate future planning for water resources, the response of precipitation to climatic change in Southern California needs to be more clearly understood. Numerous proxies have been tested for Southern California, including tree ring widths (e.g. Cook and Krusic, 2004; MacDonald, 2007), δ¹⁸O of marine planktonic foraminifera (e.g. Kennett and Kennett, 2000), pollen (e.g. Heusser and Sirocko, 1997), archeological remains (e.g. Lambert, 1994; Glassow, 2002) and flood deposit thickness (e.g. Schimmelmann et al., 2003). One new proxy that holds promise, but has not been tested in this region,

is the hydrogen isotopic composition (D/H ratio) of terrestrial leaf wax lipids.

Plants obtain all of their dietary hydrogen from environmental water, so the isotopic composition of C-bound H that is 'fixed' by these plants should reflect that of environmental water. Numerous studies of cultured plants (e.g. Zhang and Sachs, 2007), natural ecosystems (e.g. Xie et al., 2000; Sachse et al., 2006), lake core-top sediments (e.g. Huang et al., 2002, 2004; Sachse et al., 2004; Hou et al., 2006, 2008) and even surface soils (Rao et al., 2009) confirm that this is so. The D/H ratio of environmental water is in turn controlled both by that of incoming precipitation and by evapotranspiration from soils and plants (e.g. Yakir et al., 1990; Smith and Freeman, 2006; Feakins and Sessions, 2010). The D/H ratio of precipitation is also influenced indirectly by aridity because falling rain droplets partially evaporate and become D-enriched (Risi et al., 2008). All these effects tend to reinforce each other, such that environmental water becomes D-enriched in hot dry climates and D-depleted in cold wet ones. We might, therefore, expect that sedimentary records of lipid δD values would provide a record of such hydrologic changes and allow us to develop an improved understanding of the historical moisture budget of Southern California.

A significant problem for developing such records is that long lived natural lakes are rare in Southern California. While they do

* Corresponding author. Address: Department of Earth Sciences, University of California, Riverside, CA 92521, USA. Tel.: +1 951 827 3181; fax: +1 951 827 4324.
E-mail address: chaoli@ucr.edu (C. Li).

exist (e.g. Kirby et al., 2007; Blazevic et al., 2009), most now drain heavily developed or agricultural regions that would be unsuitable for core-top calibration studies. As a potential alternative, we explore here the marine Santa Barbara Basin (SBB; Fig. 1). SBB is a nearshore basin that receives a strong input of terrigeneous sediments from the Santa Ynez Mountains, contains abundant organic matter including terrestrial leaf waxes, and has rapid accumulation rates and varved sediments. It has also been heavily studied from a marine paleoclimate perspective, and long sediment archives already exist with appropriate age models. If lipids record terrestrial aridity, this would be an ideal place to develop long, high resolution proxy records.

To this end, we measured D/H ratios of putative terrestrial leaf wax lipids, including intermediate (hereafter "mid-") and long chain fatty acids (FAs) and long chain n-alkanes, from two overlapping cores spanning the present back to ca. 600 AD. Results are then compared with existing data for drought severity, based primarily on the tree ring-based winter Palmer Drought Severity Index (PDSI).

2. Regional setting

SBB is a semi-enclosed coastal basin bounded by the Santa Ynez Mountains (600–1800 m elevation) to the north and a succession of islands (San Miguel, Santa Rosa, Santa Cruz and Anacapa) to the south (Fig. 1). It is connected to the Pacific Ocean to the northwest and southeast by two sills, at 450 and 230 m water depth respectively, which limit circulation in deep waters of the basin. The resulting suboxic to anoxic conditions provide greatly enhanced preservation of both autochthonous and allochthonous organic matter (Mollenhauer and Eglinton, 2007) and promote the deposition of varved sediments in the central SBB (Schimmelmann et al., 2006).

Fluvial input to the basin is mainly from the perennial Ventura and Santa Clara Rivers (VR and SCR, respectively), which extend northeast into the continental interior of the Coastal Range (Fig. 1). Discharge from these rivers is the major contributor to terrigenous sedimentation of the SBB (Fleischer, 1972; Hein et al., 2003). Erosion in the Ventura/Santa Clara drainage system is controlled primarily by precipitation, which peaks during winter and spring (see below) and carries silt and clay-size particles into the SBB (Schimmelmann et al., 2003; Robert, 2004). Notably, the SCR is one of the largest river systems along the coast of Southern

California, and drains an area of 4100 km² in the coastal ranges. Annual sediment load for the SCR is highly variable (0.01–100×10^9 kg) and hyperpycnal transport of suspended sediment during flood events in winter and spring accounts for ca. 75% of the cumulative sediment load discharged by the SCR over the past 50 years (Warrick and Milliman, 2003). Accordingly, the SBB is a promising testing ground for using terrestrial lipids as a proxy for paleoprecipitation in the adjacent watershed.

California's climate is dominated by a semi-permanent high pressure area over the North Pacific Ocean, known as the Pacific High. This pressure center moves north during the summer, pushing storm tracks with it and resulting in little or no precipitation for the southern part of the state. During winter, the Pacific High retreats to the south, permitting storm centers to swing across Southern California, bringing most of the region's precipitation. El Niño and La Niña conditions periodically change the circulation pattern, resulting in wetter or more arid conditions, respectively. On average, the Santa Barbara area receives about 300–500 mm of precipitation annually, mostly in winter. The mild Mediterranean-type climate of the region sustains a composite vegetation of mostly grasses and oaks in the coastal plain, grading to dominant *Artemisia* brush near the coast. Chaparral-type ecosystems predominate on the region's relatively dry slopes, with juniper, oak and pine in the most elevated areas.

3. Methods

3.1. Sample collection

A composite sediment core was collected (SBB1, 34°13′N, 120°2′W; Fig. 1) at a depth of 583 m during a cruise of the R/V New Horizon in June 2004. It consisted of an upper multicore (SBB1-MC3, 67 cm) that preserved the sediment/water interface, and a gravity core (SBB1-GC2, 220 cm) that did not. The two cores were aligned vertically on the basis of porewater chemical profiles (primarily sulfate and H₂S) as described by Li et al. (2009) and Fig. 2. Sampling details and related geochemical data are reported by Li et al. (2009) and a detailed sample list can be found in the online Supplementary data Tables S1 and S2.

To examine the terrestrial origins of mid-chain FAs (C₂₂–C₂₄) preserved in the SBB cores, we collected samples of river bed sediment and dominant aquatic macrophyte plants from 3 sites along a 30 km stretch of the SCR (Table 1) in June, 2009. Sediment
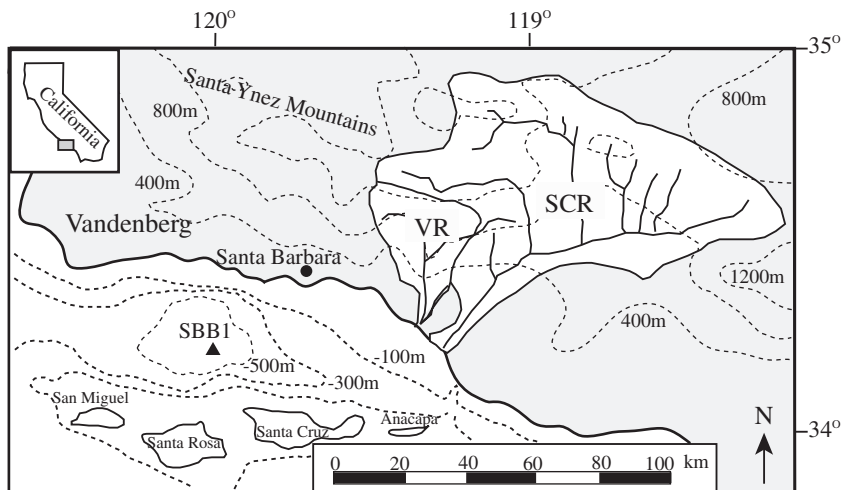

Fig. 1. Bathymetric map of Santa Barbara Basin, showing the location of core SBB1. VR: Ventura River, SCR: Santa Clara River. White areas on land define the catchments of VR and SCR. Modified from Schimmelmann et al. (2003).
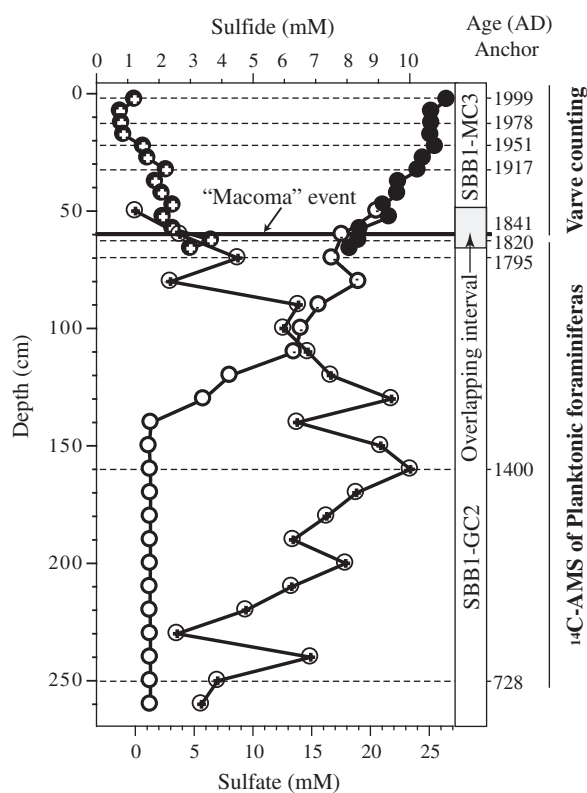
Fig. 2. Sulfide and sulfate profiles of core SBB1 showing alignment of the upper (MC3, filled circles) and lower (GC2, open circles) subcores. Measured ages are also marked.

samples were collected both from within the river channel and from (dry) overbank deposits using a shovel and stored in pre-combusted glass jars. Plant specimens included cattails (*Typha* spp.), which predominate in the estuary, and an unidentified green algal macrophyte growing submerged in the upper part of the river. Both were harvested with clean scissors, stored in plastic zip-lock bags, and transported on ice to Caltech.

3.2. Lipid extraction, purification and derivatization

Two types of common terrestrial lipids were examined: long chain *n*-alkanes and mid- to long chain *n*-alkanoic acids (FA). Extraction and purification of *n*-alkanes followed the same procedures used by Li et al. (2009), except that alkanes were obtained by silica gel chromatography (1 g, 5% deactivated). For the *n*-alkane data, 12 of 28 samples were previously reported by Li et al. (2009).

FAs were isolated by first saponifying [0.5 M NaOH (10 ml) in H_2O at 70 °C for 4 h] 4 g dried sediment, then were extracted and separated (cf. Li et al., 2009). The current samples should thus be considered as 'total' FAs, rather than 'bound' or 'free' FAs and all the data reported are new relative to Li et al. (2009).

River sediment (4 g) and plant biomass (0.5 g) samples were processed in the same way as the SBB sediments, except that we saponified total lipid extracts obtained from microwave extraction (see Li et al., 2009) rather than the dried sediments or plant tissue prior to extraction. This was necessary in order to avoid the formation of a strong emulsion for the plant samples. Extraction was carried out using the same procedure as for alkanoic acids from SBB sediments.

3.3. GC–MS and D/H analyses

Analytical methods for lipid identification, quantification and D/H measurements were identical to those in Li et al. (2009). All isotopic data are reported in the typical δD notation, in units of permil (‰) relative to the VSMOW standard. Precision and accuracy of the compound-specific δD measurements are a function of both analyte concentration and complexity of the GC chromatogram. The mean precision for replicate analyses of the external *n*-alkane standard compounds was 3.7‰ (1σ), and the root-mean-squared (RMS) error for all external standards was 3.4‰ (*n* = 570). For the long chain *n*-alkanes, a high level of precision was achieved largely because of the clean chromatographic background resulting from the urea adduction. Standard deviation (*n* ⩾ 3) for *n*-C_{27} to *n*-C_{33} was between 0.5‰ and 10.2‰, and typically <5‰ for samples where replicate analyses were available. For mid- and long chain FAs, a similar but slightly larger range of precision was obtained. Only in a few cases (e.g. $C_{26:0}$) did FA methyl ester peaks coelute with other minor components or appear at positions in the chromatogram with a variable baseline, leading to poorer precision of up to 14.6‰.

3.4. Radiocarbon dating

At least 6 mg of planktonic foraminifera were hand picked from each sediment sample for radiocarbon (^{14}C) analysis. The selected species included *Globigerina bulloides*, *Neogloboquadrina pachyderma* and *Globigerina quinqueloba*, which are abundant in SBB sediments and have been widely used for radiocarbon dating (e.g. Hendy et al., 2002). Radiocarbon measurements were performed at the National Ocean Sciences Accelerator Mass Spectrometry (NOSAMS) Facility at Woods Hole Oceanographic Institution. The foraminiferal tests were acidified under vacuum with 100% H_3PO_4 in a 60 °C bath overnight. The resulting gas was collected and purified, graphitized over an Fe catalyst and analyzed by

Table 1
FAs in SCR sediments and plants.

Sample	SCR-S1	SCR-S2	SCR-S3	SCR-P1	SCR-P2
Approximate distance to SCR outlet (km)	0	10	30	0	30
Sample matrix	Fine grained estuary sediment	Coarse grained riverbed sediment	Fine grained overbank deposit	Cattail leaves	Submerged green alga
Concentration (μg/g dry sediment or dry tissue) and δD value (‰)					
22:0	0.25(−145)	0.27(−137)	0.13(−148)	0.73(−148)	0.00
24:0	0.33(−131)	0.34(−146)	0.18(−154)	1.45(−150)	0.00
26:0	0.21(−123)	0.23(−144)	0.13(−152)	1.01(−144)	0.00
28:0	0.09(−107)	0.29(−139)	0.12(−142)	0.61(−133)	0.00
30:0	0.00	0.28(−143)	0.00	0.18	0.00
(22:0 + 24:0)/(26:0 + 28:0 + 30:0)	1.91	0.76	1.23	1.21	n/a[a]

[a] Not applicable.

AMS. The ^{14}C results are reported as conventional radiocarbon ages (Stuiver and Polach, 1977; Stuiver, 1980) and include a $\delta^{13}C$ correction for isotopic fractionation. Radiocarbon ages were calculated using 5568 years as the half life of radiocarbon and are reported without regional reservoir age (ΔR) corrections or calibration to calendar years.

3.5. Calculation of correlation coefficients (R^2)

The SBB sediment samples have inherently variable temporal resolution because the two substituent cores (multicore and gravity core) were sampled at different physical resolution (5 and 10 cm, respectively) and because compaction changes the relationship between depth and age. In contrast, the tree ring-based winter PDSI record to which our D/H records are compared (see Section 4.2) has annual resolution over the past 2000 years, with an entirely independent chronology. For quantitative comparison of the two records, the following approach was adopted. First, start and end dates for each sediment sample were calculated on the basis of the age model described in Section 4.1. Next, all PDSI values falling into that same age range (based on the tree ring chronology) were averaged. This resulted in paired δD and PDSI values and correlation coefficients could be calculated directly using Microsoft Excel. To introduce a potential time lag into the sediment chronology, representing the residence/transport time for organics into the sedimentary record, we simply adjusted the age range of all sediment samples by an integral number, recalculated the corresponding PDSI average values, and then recalculated correlation coefficients.

A similar approach was applied to correlation between the δD record and SBB marine $\delta^{18}O$ record (with 10 year age range error for data averaging) but only for zero year and 215 year time lags because of the large and variable resolution in the $\delta^{18}O$ record, typically 5–55 years over the past 1400 years (Kennett and Kennett, 2000).

For FA δD records, surface (core top) samples were excluded from the correlation analysis because of their anomalously high concentration, which potentially indicates an input of labile marine components. This omission resulted in a very minor adjustment to calculated R^2 values.

4. Results and discussion

4.1. Sediment core chronology

Accurate ages for the top four samples of SBB1-MC3 were determined on the basis of varve counts from X-radiographs (Schimmelmann et al., 2006). The top 32 cm represent 88 years of sedimentation from 1916–2004. Four deeper horizons (62.5, 70, 160 and 250 cm) were selected for ^{14}C dating to constrain the age of the remainder of the core, and are summarized in Table 2

and marked in Fig. 2. The accuracy of the stratigraphic alignment of the multicore and gravity core (Section 3.1) was confirmed by the similar ^{14}C ages of two samples located just above and below the juncture. Based on this alignment, the composite core provided a complete record of the top 260 cm of SBB sediments.

In order to avoid large age errors caused by varying marine radiocarbon reservoir age (ΔR) in SBB (Ingram and Southon, 1996), we employed the existing age model of Schimmelmann et al. (2006) for the central SBB, which is based on varve counting over the past ca. 6700 years with paired radiocarbon ages from both benthic and planktonic foraminifera. To transfer this age model to our core, we fitted the last 3200 year planktonic foram data from Schimmelmann et al. (2006) with a power function ($R^2 = 0.992$; Fig. 3A) to provide a radiocarbon 'calibration' curve. An alternative linear age model was also tested, and produced similar but slightly worse ($R^2 = 0.964$) results than the power model. Placing our foram ^{14}C ages onto this curve provides calibrated sediment ages for the SBB1 core that are tied to the original varve chronology (Fig. 3A).

The calibrated age tie points in our core are best fit ($R^2 = 0.9999$) by a polynomial interpolation for depths <160 cm, consistent with the variable effects of compaction in shallow sediments (Fig. 3B). As an independent test of this age model, we examined the appearance of the "Macoma event" in our cores. This event left a unique layer of Macoma leptonoidea pelecypod shells deposited in 1841 AD (Schimmelmann et al., 2006) and observed at a depth of 59–61 cm in our core. Our age model returns an age range of 1827–1834 AD for the Macoma layer, close to its actual depositional age. However, the polynomial age model does not fit well with the deepest sample (250 cm; Fig. 3B), suggesting that the polynomial relationship observed in the upper core due to sediment compaction gradually disappears in the lower core. In the absence of any further age control, we use a linear fit between the deepest two radiocarbon ages.

4.2. Comparison of paleoclimatic proxy records

4.2.1. Long chain FAs

Downcore variations in the δD values of long chain FAs are quite subtle and decrease in magnitude with increasing chain length (Fig. 4A–C). Standard deviations for the records are 7.9‰ (C_{26}), 4.5‰ (C_{28}), and 3.4‰ (C_{30}). The latter two values are indistinguishable from analytical precision. The mean δD values of these FAs also decrease with chain length, with C_{30} having the lowest value of $-144‰$ (Table 3). Correlation coefficients between the FA δD records and both winter PDSI and marine $\delta^{18}O$ are uniformly below 0.1 regardless of time lag, with only two exceptions (Table 3): R^2 for C_{30} δD and PDSI reaches a maximum value of 0.25 ($p < 0.05$) at a 40 year time lag (Fig. 5) and R^2 for C_{26} δD and marine $\delta^{18}O$ at a 215 year time lag has a value of 0.19 ($p < 0.05$). Given the lack

Table 2
Age control for core.

Sample	Depth range (cm)	Dating method	[14]C age (^{14}C year BP)	Error (^{14}C year)	Calendar age range (year AD)[a]	Calendar age (year AD)[a]
MC3–01	0–5	Varve counting	–	–	2004–1994	1999
MC3–03	10–15	Varve counting	–	–	1984–1971	1978
MC3–05	20–25	Varve counting	–	–	1960–1944	1951
MC3–07	30–35	Varve counting	–	–	1925–1909	1917
Macoma	59–61	Historical event	–	–	–	1841
MC3–13	60–65	^{14}C-AMS	815	30	1830–1813	1820
GC2–03	65–75	^{14}C-AMS	885	30	1813–1776	1795
GC2–12	155–165	^{14}C-AMS	1620	25	1426–1375	1400
GC2–21	245–255	^{14}C-AMS	2370	30	765–691	728

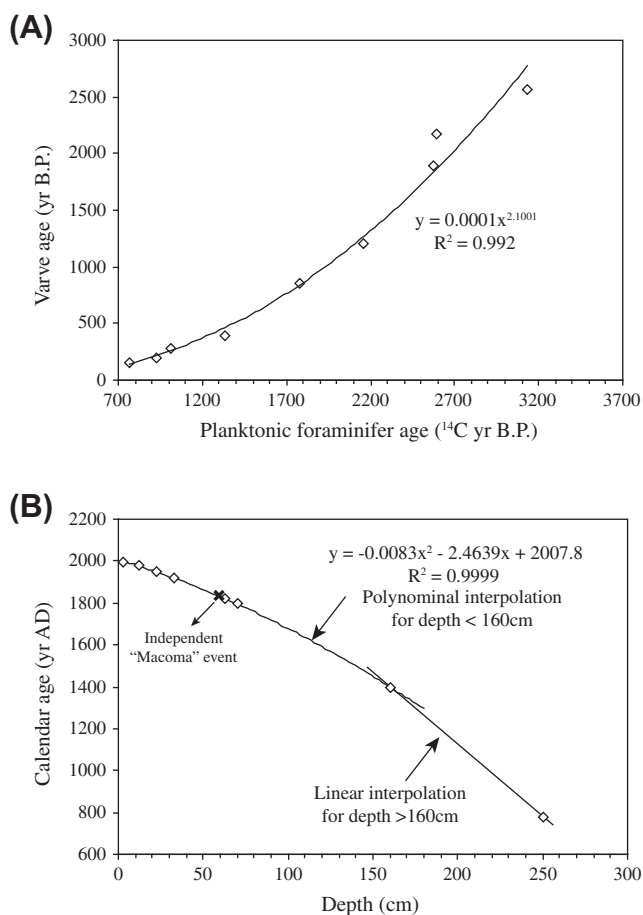[a] Measured using ^{14}C-AMS and calibrated with the power age model described in the text.

Fig. 3. Sediment core chronology. (A) Calibration dataset relating planktonic foram ^{14}C ages to varve-counted ages in SBB. Data from Schimmelmann et al. (2006). (B) Age model for the composite SBB core. See text for details.

of significant downcore variance in δD values of the FAs, these correlations are presumably artifacts of analytical noise.

Long chain FAs are thought to derive mainly from the leaf waxes of terrestrial vascular plants (e.g. Cranwell, 1974; Eglinton and Eglinton, 2008). Therefore, our data would seem to imply that the D/H values of terrestrial leaf waxes did not change significantly in this region over the past 1400 years. This is hard to reconcile with the independent winter PDSI and other climate records shown in Fig. 4 and with observations from other regions showing that δD values of modern terrestrial leaf waxes are well correlated with the δD values of precipitation (see Section 1). Two alternative explanations for the lack of variance in SBB sediments are that meteoric water δD values in the region do not covary with climate, or that climatic signals have been obscured by long term storage and mixing of lipids. Either effect would be contrary to assumptions that are commonly employed to develop leaf wax paleoproxy records.

Strong correlation of meteoric water δD and aridity has been well documented in many moist environments, particularly the tropics, where the relationship is often described as the 'amount effect' (Risi et al., 2008). However, to our knowledge this effect has never been documented in Southern California. Friedman et al. (1992) measured 7 years of monthly precipitation from 32 sites across Southern California and found no significant correlation between rainfall amount and δD values for any individual site. There was a moderate correlation between rainfall amount and δD values across all sites, but it was the inverse of that expected, i.e. lower rainfall was correlated with more negative δD values. This spurious correlation arose because temperature and aridity

increase with distance from the coast, while rainfall δD decreases because of progressive distillation of moisture from clouds as they travel inland. Fifteen years of monthly average rainfall data from the Santa Maria site of the Global Network of Isotopes in Precipitation (GNIP) database showed a moderate ($R^2 = 0.36$) correlation between rainfall amount and δD and no correlation with mean air temperature. When data are binned into annual weighted means, the correlation with amount disappears ($R^2 = 0.003$). The physical basis for this lack of correlation is likely that rainfall in Southern California is controlled mainly by the number of storms crossing the region, rather than by the amount of moisture wrung out of each storm.

D enrichment derived from evaporation of soil water and transpiration of leaf water also contributes to the climate signals in environmental water. While such processes obviously exist, two recent studies [Hou et al. (2008) in the Great Basin; Feakins and Sessions (2010) in Southern California] have both shown that their impact on leaf water in drought-adapted plants is minimal. This is presumably because most of these plants grow new leaves, and synthesize new leaf waxes, during the rainy season when evapotranspiration is minimized. In summary, existing meteorologic and plant data – which are based on monthly and annual scale variations – do not indicate a significant correlation between leaf wax δD and aridity for Southern California. The possibility that there is also little correlation on long timescales must therefore be considered.

A second possible explanation for the lack of downcore δD variation in long chain FAs is that significant mixing of terrigenous sediments, and thus lipids, occurs during their transport to the SBB basin depocenter, resulting in averaging of climate signals. $C_{26:0}$ and $C_{28:0}$ FAs from the pre-bomb horizon of the SBB depocenter have radiocarbon ages of 840 ± 80 and 1660 ± 160 years B.P., respectively (Mollenhauer and Eglinton, 2007), providing direct evidence for a long transit time and a dominance of fluvial over aeolian transport processes. Erosion and transport of sediments to the ocean is highly episodic in Southern California, with >90% of the sediment exported by the SCR occurring during flood events (Masiello and Druffel, 2001). During a series of floods in 1997–1998, the flux weighted average Δ^{14}C value for particulate organic carbon (POC) in the stream was $-428 \pm 76‰$, equivalent to 4400 calendar years. Because these measurements were obtained for bulk organic carbon, which is significantly affected by the admixture of fossil carbon from weathering of black shales, it is impossible to quantitatively predict the behavior of specific leaf wax compounds. Nevertheless, these characteristics suggest that the SCR transports and delivers to SBB a mixture of terrestrial lipids of widely varying ages, with strong averaging of climatic signals.

4.2.2. Mid-chain FAs

In contrast to the long chain FAs, mid-chain (C_{22} and C_{24}) FAs at SBB1 have δD values ranging from $-90‰$ to $-130‰$ (Fig. 4D and E) and display larger downcore variance (Table 3). Changes in δD values appear potentially related to climatic shifts, e.g. the relative D enrichments from 1050 AD to 1500 AD in the lipid record could reflect the medieval drought (850–1300 AD) recorded by other proxies (Fig. 4F–K). Correlation coefficients between the mid-chain FA δD records and the winter PDSI record are largest at a time lag of ca. 215 years (Fig. 5) with R^2 values of 0.26 ($p < 0.01$) and 0.22 ($p < 0.05$) for C_{22} and C_{24}, respectively. The δD and winter PDSI records also exhibit a second, local maximum in correlation with a time lag of 67 years (Fig. 5). Because this is approximately the time spacing between samples in the deeper SBB1 core and the significance level of these correlations is low ($p > 0.05$; Table 3), we believe this maximum is artifactual. All the correlations observed between the δD and winter PDSI records are negative, in agreement with the expected isotopic relationships, i.e. higher δD values
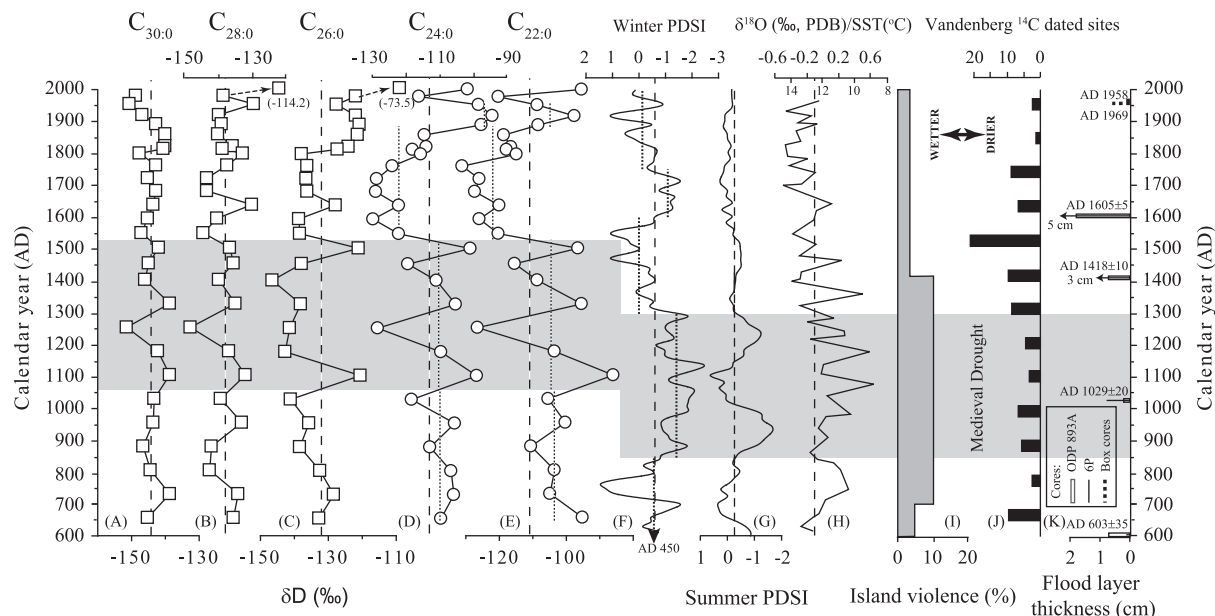
Fig. 4. Comparison of δD records of intermediate and long chain FAs preserved in SBB with independent climatological, archeological and sedimentological records from coastal Southern California for the past 1400 years. (A–E) δD records of $C_{30:0}$, $C_{28:0}$, $C_{26:0}$, $C_{24:0}$ and $C_{22:0}$, respectively. (F) Winter PDSI record of coastal Southern California (MacDonald, 2007). (G) Summer PDSI record of Southern California (grid point #48; Cook and Krusic, 2004). (H) Santa Barbara Channel sea-surface temperature (SST) record based on $\delta^{18}O$ of *G. bulloides* (Kennett and Kennett, 2000). (I) Quantitative archeological record for lethal violence on the Northern Santa Barbara Channel Islands (Lambert, 1994). (J) Frequency distribution of calibrated radiocarbon dates from Chumash sites in the Vandenberg region (Glassow, 2002). (K) Flood deposit record from central SBB sediments/cores (Schimmelmann et al., 2003). Sixty-year smoothing was applied to highlight centennial-scale changes in the winter and summer PDSI records of the coastal Southern California. The horizontal gray zone represents the Medieval Drought from about 850 AD to 1300 AD. Vertical dashed line for each record represents the mean of the record, while the short vertical dotted lines in the winter PDSI and δD records of $C_{22:0}$ and $C_{24:0}$ represent the means of potential climatic intervals in these records.

Table 3
Downcore characteristics of lipid concentration and D/H ratio in SBB cores.

Lipid	Concentration		δD		Max ± R of δD vs. winter PDSI[b]		R of δD vs. SBB foram $\delta^{18}O$ [b]	
	Average (μg/g)	Loss (%) in top 42.5 cm[a]	Avg. (‰)	SD	<150 (FAs) or <20 (alkanes) year delay	150–400 (FAs) or 20–150 (alkanes) year delay	0 year delay	215 year delay
n-FA								
22:0	0.79	78	−111.3	11.8	−0.27 (27)	−0.51 (27;<0.01)	0.53 (26;<0.01)	0.13 (27)
24:0	1.36	82	−113.3	10.3	−0.19 (27)	−0.47 (27;<0.05)	0.29 (26)	−0.08 (27)
26:0	1.36	87	−132.3	7.9	0.01 (27)	−0.26 (27)	−0.22 (26)	−0.43 (27,<0.05)
28:0	0.63	54	−138.1	4.5	−0.19 (27)	−0.11 (27)	0.19 (26)	−0.05 (27)
30:0	0.33	52	−144.0	3.4	−0.46 (27;<0.05)	−0.21 (27)	0.14 (26)	0.22 (27)
n-Alkane								
n-C23	0.10	33	−127.4	17.1	n.c.[c]	n.c.	n.c.	n.c.
n-C25	0.11	45	−150.2	11.2	n.c.	n.c.	n.c.	n.c.
n-C27	0.40	39	−156.8	10.7	−0.90 (9;<0.01)	0.64 (9)	−0.27 (26)	−0.06 (27)
n-C28	0.14	15	−128.3	14.2	−0.97 (6;<0.01)	0.76 (6)	n.c.	n.c.
n-C29	1.46	32	−155.6	8.8	−0.81 (9;<0.01)	0.57 (9)	0.31 (26)	0.15 (27)
n-C31	1.06	38	−155.6	8.2	−0.79 (9;<0.05)	0.62 (9)	0.15 (26)	0.20 (27)
n-C33	0.60	35	−151.3	11.8	−0.69 (9;<0.05)	0.63 (9)	−0.06 (26)	−0.02 (27)

[a] Calculated as $100 \times (C_{2.5cm} - C_{<42.5cm})/C_{2.5cm}$, where C is concentration and $C_{<42.5cm}$ is abundance mean for samples in depth <42.5 cm.
[b] Data given as R (n; p) but R(n) when p > 0.05.
[c] Not calculated because too few data points are available.

during drier periods (Feakins and Sessions, 2010). There is no significant correlation with summer PDSI records (Fig. 4G), consistent with the fact that most rainfall occurs during January–March in this region.

Somewhat surprisingly, the C_{22} FA is also moderately correlated with the marine $\delta^{18}O$ record, with $R^2 = 0.28$ ($p < 0.01$) at zero time lag (Table 3). The C_{24} FA is not appreciably correlated with marine $\delta^{18}O$ ($R^2 = 0.08$) at zero time lag, nor is either FA correlated with marine $\delta^{18}O$ at a time lag of 215 years ($R^2 = 0.02$ and 0.01, respectively). The correlation of C_{22} with marine $\delta^{18}O$ is thus not the result of simple covariance between the marine $\delta^{18}O$ and winter PDSI records. It would, however, be consistent with a partial marine

source for that FA, presumably benthic heterotrophic bacteria (Craven and Jahnke, 1992).

The origins of the C_{22} and C_{24} FAs are thus somewhat uncertain. They are commonly attributed to terrestrial aquatic plants (Ficken et al., 2000), a view subscribed to by Li et al. (2009) on the basis that mid-chain acids in SBB are D enriched by ca. 30‰ relative to other marine phytoplanktonic products. However, our new data show that they are also enriched by ca. 30‰ relative to SCR sediments and plants (Table 1), making this explanation incomplete at best. The abundance ratios of mid- to long chain FAs are roughly the same in SBB sediments (0.6–1.3; Table S1) as in SCR sediments (0.7–1.9; Table 1), favoring a terrestrial
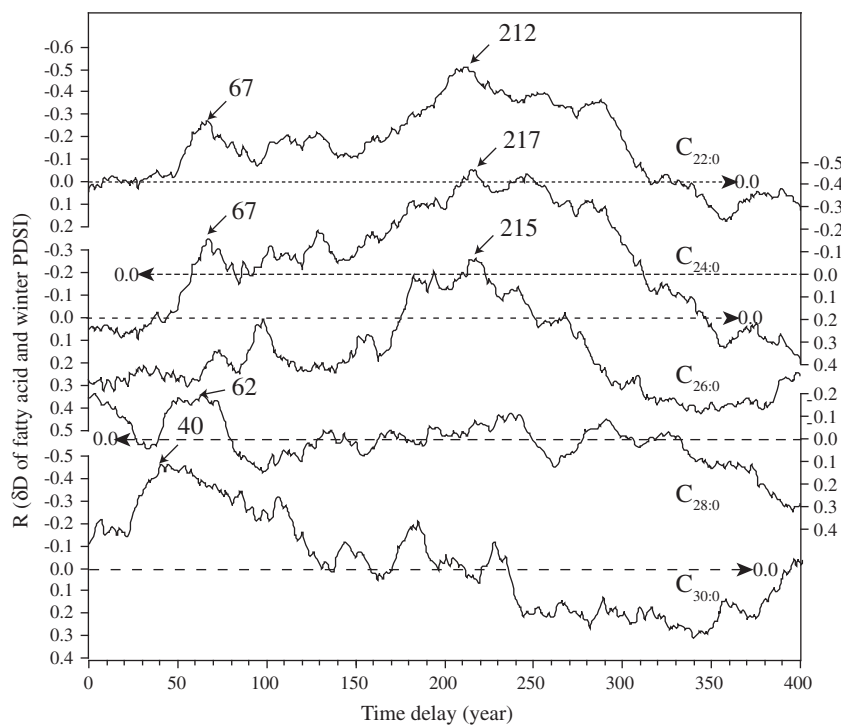
Fig. 5. Correlation coefficients (R) between fatty acid δD records and winter PDSI as a function of inferred time lag between plant growth and sedimentation (x-axis). Horizontal dashed lines indicate R = 0 for each compound.
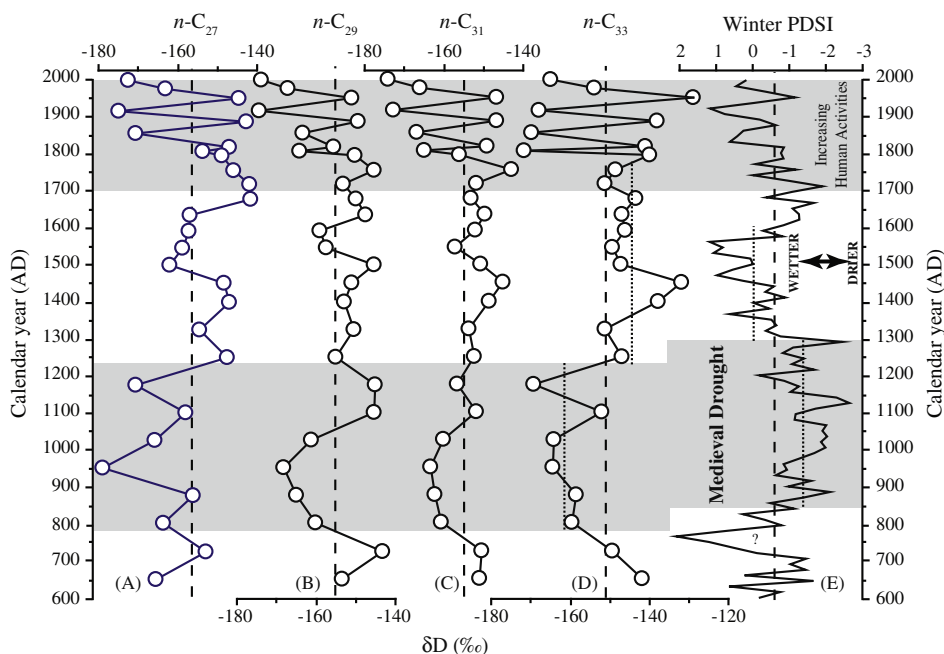

Fig. 6. Comparison of δD records of long chain alkanes (A–D: C_{27}, C_{29}, C_{31} and C_{33}, respectively) in SBB with independent winter PDSI record from coastal Southern California (E; MacDonald, 2007) for the past 1400 years. To match the multi-decadal oscillations in δD records between 1700 AD and 2000 AD, thirty-year smoothing was applied to highlight the multi-decadal changes in the winter PDSI record. Gray boxes highlight periods of greatly increased δD variability (upper box) and the medieval drought (lower box). Vertical dashed line for each record represents the mean of the record, while two short vertical dotted lines in δD record of n-C_{33} represent the means between 800 and between 1250 AD (−161.4‰) and between 1250 and 1750 AD (−145.5‰).

origin. The concentrations of C_{22} and C_{24} drop more sharply at the top of the SBB core than do longer chain acids (Table 3), suggesting a labile marine origin.

In summary, the mid-chain FAs in SBB sediments exhibit downcore variation in δD potentially related to both terrestrial climate and marine circulation, in contrast to the long chain FAs. We

hypothesize that the mid-chain FA δD values record some combination of variable mixing between two different sources, as well as changes in the terrestrial end member composition arising from climate. While it may be possible to extract some useful climate information from this archive on longer timescales, it will be a very difficult signal to interpret quantitatively.

4.2.3. Long chain n-alkanes

The δD values of long chain n-alkanes from SBB sediments show pronounced variation over the past 1400 years (Fig. 6A–D and Table 3). Samples from 800 to 1100 AD are somewhat D depleted, while the interval 1750–2000 is marked by very strong, rapid fluctuations. Average δD values are between $-150‰$ and $-157‰$, consistent with that expected for terrestrial leaf waxes (e.g. Chikaraishi and Naraoka, 2003; Bi et al., 2005). However, the large variation in δD records of the long chain n-alkanes versus those of long chain FAs (see Section 4.2.1) suggests that the n-alkanes do not derive solely from plant leaf waxes. The discrepancy is likely caused by an input of fossil hydrocarbons to SBB sediments, as indicated by an abundant unresolved complex mixture (UCM; Li et al., 2009) and the presence of D-enriched even n-alkanes (Table 3). Southern California borderland basins receive hydrocarbons from both natural petroleum seepage and, since the 18th century, anthropogenic spills (Eganhouse and Venkatesan, 1993). Moreover, fossil hydrocarbons are likely contributed by the weathering of organic-rich rocks, particularly the Miocene Monterey Shale (Petsch et al., 2000).

The n-alkane data from before and after 1700 AD are qualitatively different, with the later period recording high frequency variation not evident in earlier samples. For quantitative correlation

analysis, we therefore consider these two intervals separately. Over the period 600–1700 AD, the δD values for C_{27}, C_{29}, and C_{31} n-alkanes are only slightly correlated with winter PDSI, with no distinct maximum in correlation at any time lag between 0 and 400 years (Fig. 7A). There is, consequently, no apparent retention of climatic information. Given that the leaf wax FAs show virtually no downcore changes in δD, changes in n-alkane δD are likely attributable to varying inputs of petrogenic and/or fossil n-alkanes. It is possible that this mixing does include a climatic component, in that the erosion and sedimentation of fossil n-alkanes from organic-rich rocks is driven by precipitation and runoff. For example, the C_{33} n-alkane is less abundant than others, yet exhibits stronger downcore variation in δD (Table 3) and a stronger correlation with winter PDSI (Fig. 7A). The varying inputs of petrogenic and/or fossil n-alkanes may have a disproportionately larger effect on this less abundant compound. But in any case, none of the long chain n-alkanes appear particularly promising as paleoclimate archives.

In contrast, the n-alkane δD records from 1700 to 2000 AD are quite strongly correlated with winter PDSI, with R^2 values up to $0.81(p < 0.01; n = 9)$. However, depending on the time lag assumed, either a negative (ca. 5 year lag and $p < 0.05$; Fig. 7B) or positive (ca. 35 year lag and $p > 0.05$; Fig. 7B) correlation can be inferred. Given that δD values fluctuate at nearly the same frequency as our
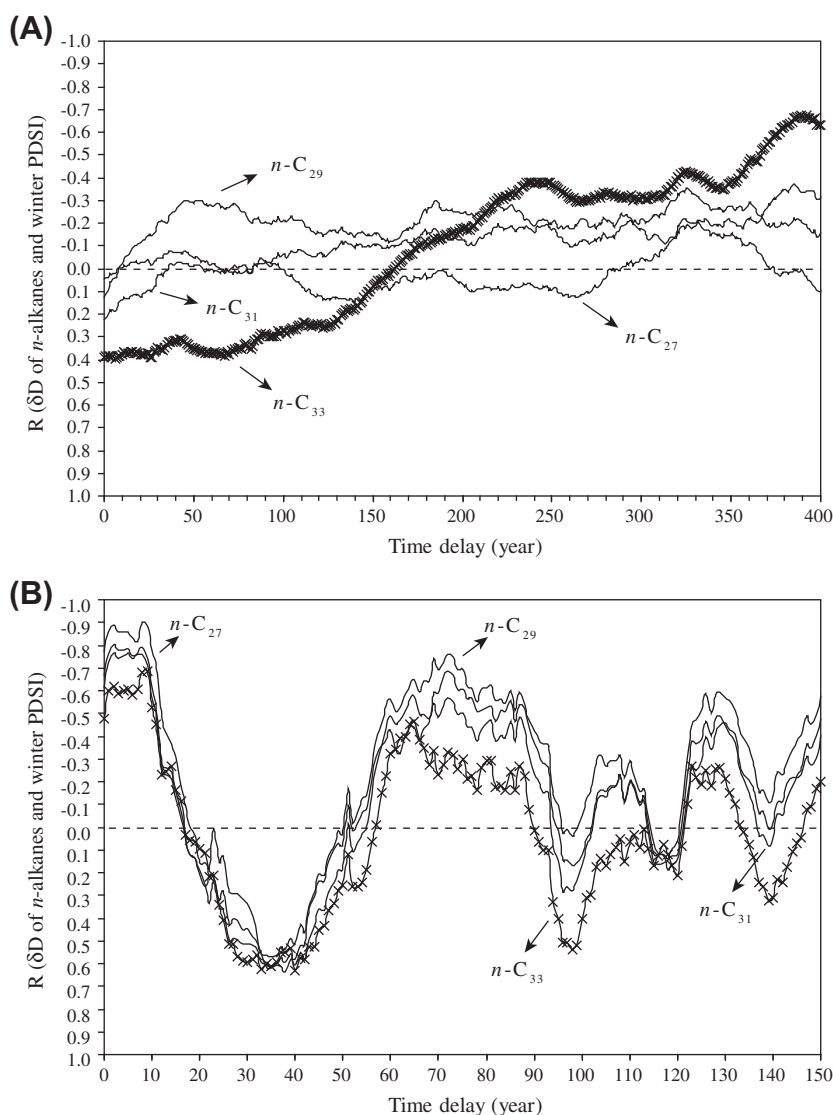

Fig. 7. Correlation coefficient (R) between n-alkane δD records and winter PDSI record as a function of inferred time lag: (A) 600–1700 AD and (B) 1700–2000 AD.

sampling interval, it is quite possible that this correlation is simply an artifact of sampling resolution. Even if it is not, the fact that it does not extend back beyond ca. 1700 AD means it is of very limited practical use. A more interesting question is why the character of the *n*-alkane δD record changes so dramatically after ca. 1700 AD, whereas there is no equivalent shift in any of the other climate proxies. It seems significant that this time period corresponds roughly to the arrival of European settlers to the California coast about 300 years ago (Chapman, 1916), with a concomitant increase in land disturbance resulting from agriculture and settlements after that. These activities perhaps facilitated more episodic erosion and delivery of fossil hydrocarbons to the SBB, leading to the more highly variable signal we observe. If so, *n*-alkane δD records might find some use as a qualitative proxy for human-induced land disturbance along other coastal margins.

4.3. Relevance for paleoclimate records

Our results from SBB raise three cautionary notes that are relevant to leaf wax paleoclimate records more generally. First, it is widely assumed that the δD value of mean annual precipitation strongly covaries with both temperature and rainfall amount, and that this signal should be transferred to plant leaf waxes. This assumption is ultimately based on the observation that precipitation δD varies with *spatial* climate gradients, and the assumption that this relationship can be reliably transferred to *temporal* climate gradients (e.g. Jouzel et al., 2000; Huang et al., 2002; Sachse et al., 2004; Hou et al., 2008). Our brief review of existing precipitation isotope data for Southern California indicates that this may be a poor assumption for some mid-latitude regions, particularly in Mediterranean-type climates where drought-adapted plants grow only during the rainy season.

Second, it is also widely assumed that transport of leaf waxes to lakes and marginal marine basins is dominantly aeolian, and thus always has the potential to record climate with high temporal resolution. Our study of the SBB indicates that this assumption may not be true for all settings. Existing radiocarbon data demonstrate that leaf wax components in SBB have a long transport time (Mollenhauer and Eglinton, 2007), consistent with similar lessons from some other marine settings (e.g. Eglinton et al., 1997; Ohkouchi et al., 2002; Mollenhauer and Eglinton, 2007) and the nearly invariant FA δD records support the idea that there is very significant mixing on ca. 1000 year timescales in SBB. We thus suggest that other future studies of leaf waxes in large lakes and marine basins should consider the transport time of leaf wax compounds into the sedimentary record, ideally through radiocarbon dating.

Third, mid-chain FAs are commonly inferred to derive exclusively from aquatic macrophyte plants (Ficken et al., 2000). Our data from SBB strongly suggest an additional source, possibly marine benthic microbial mats. It remains unclear whether a similar source might exist in large lakes, so we suggest that the origins of these compounds be treated with some caution.

5. Summary

We developed a ca. 1400 year record of δD values for *n*-alkanes and FAs derived from terrestrial plants and buried in sediments of the Santa Barbara Basin (SBB). Of the biomarkers examined, C_{22} and C_{24} FAs – both attributed at least in part to terrestrial aquatic plants – show the best correlation with winter drought. They reach a maximum correlation coefficient (R^2) of only 0.25 compared to the winter PDSI record, with an assumed temporal lag of 215 years. We interpret this lag as reflecting the transport time of lipids to the SBB depocenter, though this remains to be directly tested. In contrast, long chain FAs and *n*-alkanes derived from terrestrial plant leaf waxes do not show any significant correlation with other climate proxies. Given these relationships, the SBB does not appear promising as an archive for organic paleoproxy records on centennial timescales. We suggest that the lack of climate signals in these proxies is related mainly to long residence times for compounds in terrestrial soils and on the basin flanks, combined with sporadic deep erosion of old soils during episodic storms that results in strong mixing. If so, the SBB may still contain useful archives of terrestrial climate change on greater than millennial timescales. An alternative possibility, which needs to be evaluated, is that the isotopic composition of meteoric waters in Southern California does not strongly covary with climate.

Appendix A. Supplementary material

Supplementary data associated with this article can be found, in the online version, at doi:10.1016/j.orggeochem.2010.09.011.

Associate Editor—**S. Schouten**

References

Barnett, T.P., Pierce, D.W., Hidalgo, H.G., Bonfils, C., Santer, B.D., Das, T., Bala, G., Wood, A.W., Nozawa, T., Mirin, A.A., Cayan, D.R., Dettinger, M.D., 2008. Human-induced changes in the hydrology of the western United States. Science 319, 1080–1083.

Bi, X.H., Sheng, G.Y., Liu, X.H., Li, C., Fu, J.M., 2005. Molecular and carbon and hydrogen isotopic composition of *n*-alkanes in plant leaf waxes. Organic Geochemistry 36, 1405–1417.

Blazevic, M.A., Kirby, M.E., Woods, A.D., Browne, B.L., Bowman, D.D., 2009. A sedimentary facies model for glacial-age sediments in Southern California: Baldwin Lake, CA. Sedimentary Geology 219, 151–168.

Chapman, C.E., 1916. The Founding of Spanish California. The Macmillan Company, New York.

Chikaraishi, Y., Naraoka, H., 2003. Compound-specific δD–δ^{13}C analyses of *n*-alkanes extracted from terrestrial and aquatic plants. Phytochemistry 63, 361–371.

Cook, E.R., Krusic, P.J., 2004. The North American Drought Atlas: grid point 48. Lamont-Doherty Earth Observatory and the National Science Foundation. <http://www.l.ldeo.columbia.edu/SOURCES/.LDEO/.TRL/.NADA2004/.pdsi-atlas.html> (accessed 22.09.10).

Cranwell, P.A., 1974. Monocarboxylic acids in lake sediments: indicators, derived from terrestrial and aquatic biota, of paleoenvironmental trophic levels. Chemical Geology 14, 1–14.

Craven, D.B., Jahnke, R.A., 1992. Microbial utilization and turnover of organic carbon in Santa Monica Basin sediments. Progress in Oceanography 30, 313–333.

Eganhouse, R.P., Venkatesan, M.I., 1993. Chemical oceanography and geochemistry. In: Dailey, M.D., Reish, D.J., Anderson, J.W. (Eds.), Ecology of the Southern California Bight a Synthesis and Interpretation. University of California Press, Berkeley, pp. 71–171.

Eglinton, T.I., Eglinton, G., 2008. Molecular proxies for paleoclimatology. Earth and Planetary Science Letters 275, 1–16.

Eglinton, T.I., Benitez-Nelson, B.C., Pearson, A., McNichol, A.P., Bauer, J.E., Druffel, E.R.M., 1997. Variability in radiocarbon ages of individual organic compounds from marine sediments. Science 277, 796–799.

Feakins, S.J., Sessions, A.L., 2010. Controls on the D/H ratios of plant leaf waxes in an arid ecosystem. Geochimica et Cosmochimica Acta 74, 2128–2141.

Ficken, K.J., Li, B., Swain, D.L., Eglinton, G., 2000. An *n*-alkane proxy for the sedimentary input of submerged/floating freshwater aquatic macrophytes. Organic Geochemistry 31, 745–749.

Fleischer, P., 1972. Mineralogy and sedimentary history, Santa Barbara Basin, California. Journal of Sedimentary Petrology 42, 49–58.

Friedman, I., Smith, G.I., Gleason, J.D., Warden, A., Harris, J.M., 1992. Stable isotope composition of waters in southeastern California. 1. Modern precipitation. Journal Geophysical Research Atmosphere 97, 5795–5812.

Glassow, M.A., 2002. Late Holocene prehistory of the Vandenberg region. In: Erlandson, J.M., Jones, T.L. (Eds.), Catalysts to Complexity: Late Holocene Societies of the California Coast. Cotsen Institute of Archaeology, UCLA, Los Angeles, CA, pp. 183–204.

Hein, J.R., Dowling, J.S., Schuetze, A., Lee, H.J., 2003. Clay–mineral suites, sources, and inferred dispersal routes: Southern California continental shelf. Marine Environmental Research 56, 79–102.

Hendy, I.L., Kennett, J.P., Roark, E.B., Ingram, B.L., 2002. Apparent synchroneity of submillennial scale climate events between Greenland and Santa Barbara Basin, California from 30–10 ka. Quaternary Science Review 21, 1167–1184.

Heusser, L.E., Sirocko, F., 1997. Millennial pulsing of environmental change in southern California from the past 24 k.y.: a record of Indo-Pacific ENSO events? Geology 25, 243–246.

Hou, J., Huang, Y., Wang, Y., Shuman, B., Oswald, W.W., Faison, E., Foster, D.R., 2006. Postglacial climate reconstruction based on compound-specific D/H ratios of fatty acids from Blood Pond, New England. Geochemistry, Geophysics Geosystem 7, Q03008. doi:10.1029/2005GC001076.

Hou, J., D'Andrea, W.J., Huang, Y., 2008. Can sedimentary leaf waxes record D/H ratios of continental precipitation? Field, model, and experimental assessments. Geochimica et Cosmochimica Acta 72, 3503–3517.

Huang, Y., Shuman, B., Wang, Y., Webb III, T., 2002. Hydrogen isotope ratios of palmitic acid in lacustrine sediments record late Quaternary climate variations. Geology 30, 1103–1106.

Huang, Y., Shuman, B., Wang, Y., Webb III, T., 2004. Hydrogen isotope ratios of individual lipids in lake sediments as novel tracers of climatic and environmental change: a surface sediment test. Journal of Paleolimnology 31, 363–375.

Ingram, B.L., Southon, J.R., 1996. Reservoir ages in eastern Pacific coastal and estuarine waters. Radiocarbon 38, 573–582.

Jouzel, J., Hoffmann, G., Koster, R.D., Masson, V., 2000. Water isotopes in precipitation: data/model comparison for present-day and past climates. Quaternary Science Reviews 19, 363–379.

Kennett, D.J., Kennett, J.P., 2000. Competitive and cooperative responses to climatic instability in Southern California. American Antiquity 65, 379–395.

Kirby, M.E., Lund, S.P., Anderson, M.A., Bird, B.W., 2007. Insolation forcing of Holocene climate change in Southern California: a sediment study from Lake Elsinore. Journal of Paleolimnology 38, 395–417.

Lambert, P.M., 1994. War and peace on the Western Front: A study of violent conflict and its correlates in prehistoric hunter–gatherer societies of Coastal Southern California. Ph.D. Dissertation. University of California, Santa Barbara.

Li, C., Sessions, A.L., Kinnaman, F.S., Valentine, D.L., 2009. Hydrogen-isotopic variability in lipids from Santa Barbara Basin sediments. Geochimica et Cosmochimica Acta 73, 4803–4823.

MacDonald, G.M., 2007. Severe and sustained drought in Southern California and the west: present conditions and insights from the past on causes and impacts. Quaternary International 173–174, 87–100.

Masiello, C.A., Druffel, E.R.M., 2001. Carbon isotope geochemistry of the Santa Clara River. Global Biogeochemical Cycles 15, 407–416.

Mollenhauer, G., Eglinton, T.I., 2007. Diagenetic and sedimentological controls on the composition of organic matter preserved in California Borderland Basin sediments. Limnology and Oceanography 52, 558–576.

Ohkouchi, N., Eglinton, T.I., Keigwin, L.D., Hayes, J.M., 2002. Spatial and temporal offsets between proxy records in a sediment drift. Science 298, 1224–1227.

Overpeck, J., Udall, B., 2010. Dry times ahead. Science 328, 1642–1643.

Petsch, S.T., Berner, R.A., Eglinton, T.I., 2000. A field study of the chemical weathering of ancient sedimentary organic matter. Organic Geochemistry 31, 475–487.

Rao, Z., Zhu, Z., Jia, G., Henderson, A.C.G., Xue, Q., Wang, S., 2009. Compound specific δD values of long chain *n*-alkanes derived from terrestrial higher plants are indicative of the δD of meteoric waters: evidence from surface soils in eastern China. Organic Geochemistry 40, 922–930.

Risi, C., Bony, S., Vimeux, F., 2008. Influence of convective processes on the isotopic composition ($\delta^{18}O$ and δD) of precipitation and water vapor in the tropics: 2. Physical interpretation of the amount effect. Journal of Geophysical Research 113, D19306. doi:10.1029/2008JD009943.

Robert, C., 2004. Late Quaternary variability of precipitation in Southern California and climatic implications: clay mineral evidence from the Santa Barbara Basin, ODP Site 893. Quaternary Science Reviews 23, 1029–1040.

Sachse, D., Radke, J., Gleixner, G., 2004. Hydrogen isotope ratios of recent lacustrine sedimentary *n*-alkanes record modern climate variability. Geochimica et Cosmochimica Acta 68, 4877–4889.

Sachse, D., Radke, J., Gleixner, G., 2006. δD values of individual *n*-alkanes from terrestrial plants along a climatic gradient – implications for the sedimentary biomarker record. Organic Geochemistry 37, 469–483.

Schimmelmann, A., Lange, C.B., Meggers, B.J., 2003. Paleoclimatic and archaeological evidence for a 200-yr recurrence of foods and droughts linking California, Mesoamerica and South America over the past 2000 years. The Holocene 13, 763–778.

Schimmelmann, A., Lange, C.B., Roark, E.B., Ingram, B.L., 2006. Resources for paleoceanographic and paleoclimatic analysis: a 6700-year stratigraphy and regional radiocarbon reservoir-age (ΔR) record based on varve counting and ^{14}C-AMS dating for the Santa Barbara Basin, offshore California, USA. Journal of Sedimentary Research 76, 74–80.

Smith, F.A., Freeman, K.H., 2006. Influence of physiology and climate on δD of leaf wax *n*-alkanes from C_3 and C_4 grasses. Geochimica et Cosmochimica Acta 70, 1172–1187.

Stuiver, M., 1980. Workshop on ^{14}C data reporting. Radiocarbon 22, 964–966.

Stuiver, M., Polach, H.A., 1977. Discussion: reporting of ^{14}C data. Radiocarbon 19, 355–363.

Warrick, J.A., Milliman, J.D., 2003. Hyperpycnal sediment discharge from semiarid Southern California Rivers: implications for coastal sediment budgets. Geology 31, 781–784.

Xie, S., Nott, C., Avsejs, L., Volders, F., Maddy, D., Chambers, F., Gledhill, A., Carter, J., Evershed, R., 2000. Palaeoclimate records in compound-specific δD values of a lipid biomarker in ombotrophic peat. Organic Geochemistry 31, 1053–1057.

Yakir, D., Deniro, M.J., Gat, J.R., 1990. Natural deuterium and ^{18}O enrichment in leaf water of cotton plants grown under wet and dry conditions – evidence for water compartmentation and its dynamics. Plant, Cell and Environment 13, 49–56.

Zhang, Z., Sachs, J.P., 2007. Hydrogen isotope fractionation in freshwater algae: I Variations among lipids and species. Organic Geochemistry 38, 582–608.